Three-Dimensional Effects on Openings of Laterally Loaded Pierced Shear Walls

Can Balkaya, M.ASCE,[1] and Erol Kalkan, S.M.ASCE[2]

Abstract: Current design provisions comprise broadly described information for the detailing of reinforcement around the openings of pierced shear walls. To address this deficiency, the load capacity and stress distribution around the openings were analyzed by conducting three-dimensional (3D) nonlinear pushover analyses on typical shear wall dominant building structures. The diaphragm flexibility, behavior of transverse walls and slab-wall interaction during the 3D action were investigated in addition to effects of 3D and 2D modeling on the capacity evaluation. An effort was spent to illuminate the significance of different size and location of openings within the pierced walls having variable reinforcement ratios. The results of this study indicated that the stress flow and crack patterns around the openings of the 3D cases were drastically different than those computed for the 2D cases. The tension–compression coupling effects caused by the wall-to-wall and wall-to-slab interactions provided a significant contribution for increasing the global lateral resistance.

DOI: 10.1061/(ASCE)0733-9445(2004)130:10(1506)

CE Database subject headings: Shear walls; Openings; Lateral loads; Finite elements; Inelastic action.

Introduction

Shear wall dominant buildings constructed by using a tunnel form system (i.e., box system), so called tunnel form buildings, utilize all wall and slab elements as primary load carrying and transferring members. Unlike conventional reinforced concrete (RC) buildings, tunnel form buildings do not constitute beams and columns in their structural integrity. Its typical implementation and constructive details are exhibited in Fig. 1. In tunnel form buildings, walls and slabs having almost the same thickness are cast simultaneously. This significantly reduces the assembly time. The simultaneous casting of walls and slabs results in monolithic structures, and increases their seismic vulnerability by minimizing cold-joint formations in the most probable plastic hinge locations, such as around openings and base of shear walls. In addition to considerable resistance of tunnel form buildings against seismic loads, the speed and ease of construction make them preferable as the multistory public and residential buildings.

Despite the potential of shear-wall dominant systems against earthquake loads, cutouts to provide the functional use in shear walls may alter the force distribution significantly. However, in the literature, no analytical or experimental study utilizing the three-dimensional (3D) models either in a linear or a nonlinear fashion has been directed to the investigation of the effects of openings within pierced shear walls. The current approach given in design provisions for detailing of reinforcement around openings is generally based on the results derived from the two-dimensional (2D) analyses. The available studies only considered the 2D effects of openings. In 1958, Benjamin and Williams observed high stress concentrations around the openings in their experiments (Benjamin and Williams 1958). In this previous research, one story shear walls with different opening sizes and reinforcement details were tested at the Stanford Univ. Subsequent investigations have been concentrated on the inelastic behavior of the shear walls with openings subjected to monotonic (Yamada et al. 1974; Matsui and Ogawa 1979; Seya and Matseri 1979) and cyclic loadings (Daniel et al. 1986; Ali and Wight 1991). Different locations of openings have been considered, including those centrally placed (Daniel et al. 1986), staggered (Ali and Wight 1991), and doors located at the edges of the shear walls (Arvidsson 1974). In 1989, Ohtani investigated a design method for the crack control around the corners of the window openings (Ohtani 1989). In general, studies considering shear wall openings concentrated on coupling beam effects between adjacent shear walls. However, lack of such beams, as is the case in the tunnel form buildings, may require a different approach for their analysis and reinforcement detailing.

In the tunnel form construction technique, slabs are generally supported only along their three sides with shear walls while one side remained unsupported in order to take the formwork back after concrete casting (Fig. 1). In common practice, these three shear walls contain at least one opening for functional use and access. In this study, the stress development and their distribution around these types of wall openings were investigated by focusing on the effects of transverse walls, their contribution to the general behavior, and influence of slab–wall interaction. The tool used for that purpose is the capacity evaluation that forms the backbone of capacity design where the limiting capacity (i.e., ultimate plastic level) of the structure is evaluated. Generally and commonly the estimation of inelastic deformation demands of structural members is often accomplished by performing nonlinear static procedures (i.e., pushover procedures) in which a model

[1]Associate Professor, Dept. of Civil Engineering, Middle East Technical Univ., 06531 Ankara, Turkey. E-mail: cbalkaya@metu.edu.tr

[2]PhD Student, Dept. of Civil and Environmental Engineering, Univ. of California Davis, Davis, CA 95616 (corresponding author). E-mail: ekalkan@ucdavis.edu

Note. Associate Editor: Enrico Spacone. Discussion open until March 1, 2005. Separate discussions must be submitted for individual papers. To extend the closing date by one month, a written request must be filed with the ASCE Managing Editor. The manuscript for this paper was submitted for review and possible publication on November 7, 2002; approved on October 27, 2003. This paper is part of the ***Journal of Structural Engineering***, Vol. 130, No. 10, October 1, 2004. ©ASCE, ISSN 0733-9445/2004/10-1506–1514/$18.00.

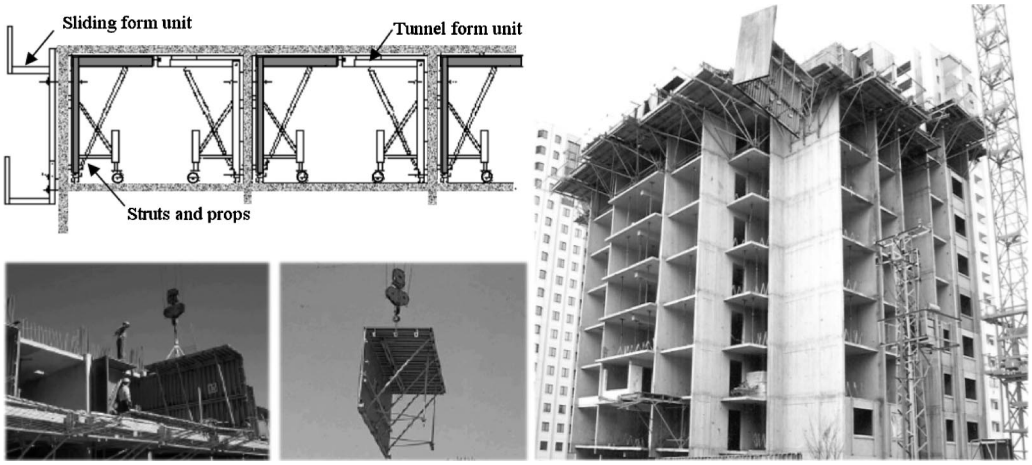

Fig. 1. Tunnel form construction technique and its special formwork system

of the building structure is subjected to an invariant distribution of lateral forces. While these procedures take into consideration redistribution of forces following yielding of sections, they do not incorporate the effects of varying dynamic characteristics during the inelastic response. Therefore nonlinear static procedure suffers from a major drawback in that it is restricted with a single mode response. However they are mostly sufficient for low-rise buildings where higher mode contribution to response can be negligible (Kunnath 2004). Therefore 3D and 2D pushover analyses based on invariant load distributions (inverted triangle) were conducted on representative two- and five-story buildings. The analyses were employed considering the effects of variable size and location of openings, and their effects to the shear flow. The nonlinear 2D and 3D finite element analyses results were compared to illuminate their differences, and highlight the significance of 3D effects. In the final part, discussion for the amount and location of the main reinforcement needed around the openings of the pierced shear walls were presented. The analytical modeling, assumptions and approach besides the results of the analyses complementing this work are summarized in the remaining sections of this paper.

Analytical Model Development

By way of evaluating the 3D and 2D nonlinear capacity of shear wall dominant RC building structures, two- and five-story residential type buildings were modeled in finite element domain. A detailed description of their plan and sections is displayed in Fig. 2. Their structural systems are composed of only shear walls and slabs having the same thickness (12 cm) as usual applications. All

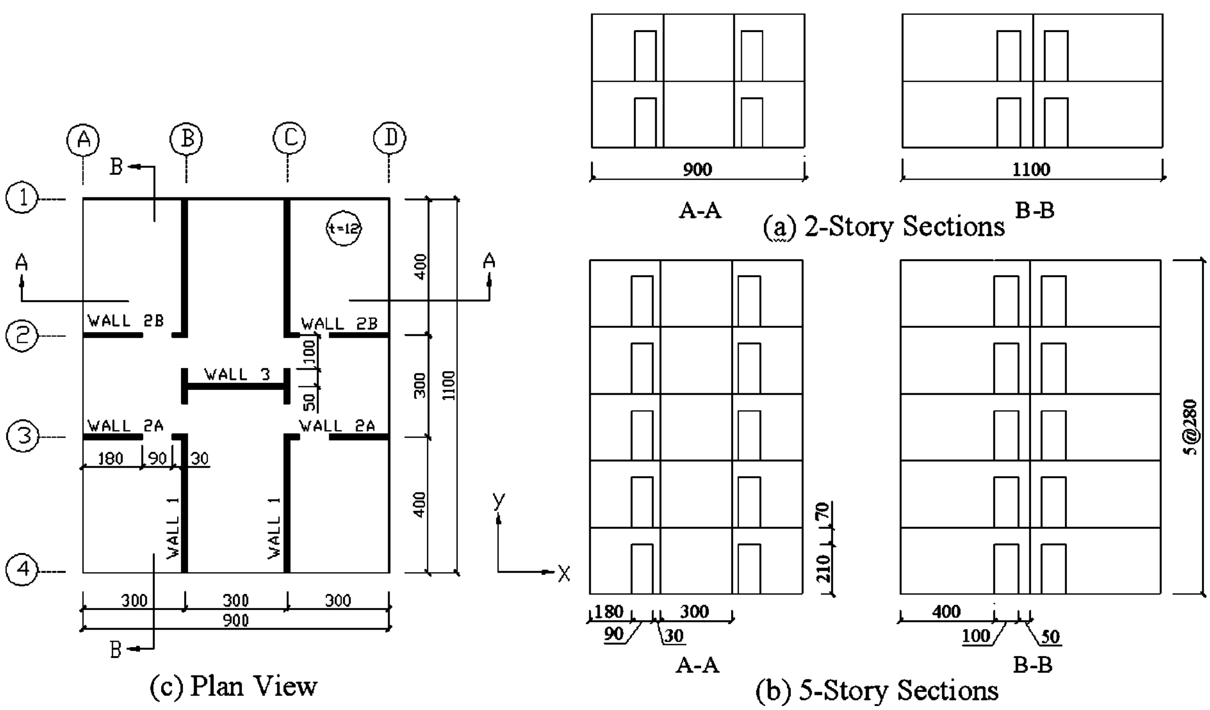

Fig. 2. Typical plan and section views for two- and five-story buildings (units are in cm)

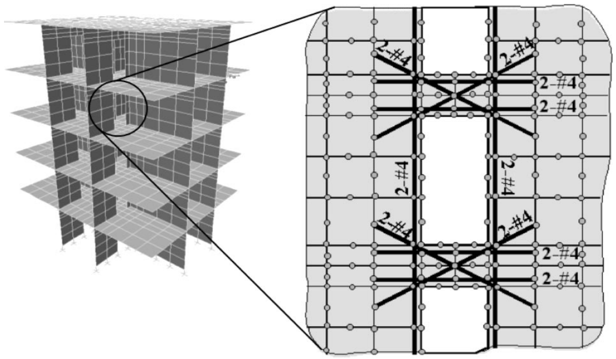

Fig. 3. Three-dimensional finite element modeling of five-story building, and its edge and diagonal reinforcement detailing around openings

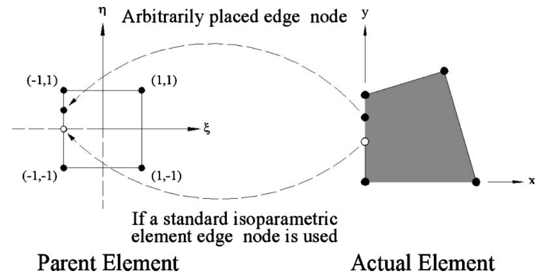

Fig. 4. One-to-one mapping between nodes of parent and actual element

of the intended lateral strength and stiffness of these buildings reside in the interior shear walls with the contribution of the slabs. In addition to their resistance to lateral loads, these distributed walls in the plan were also designed to carry gravity loads.

It is of significance to note that almost equal slab and wall thicknesses in tunnel form buildings, less than that of conventional RC structures, may result in a higher slab–wall interaction. Therefore making a rigid diaphragm assumption (infinitely rigid in their own plane) to simplify the analyses and save from the run-time may not represent their real behavior. In fact, tunnel form buildings behave like thin-wall-tubular structures where in-plane rigidity is low (Balkaya and Kalkan 2003a). Thus the high stress concentration may increase the crack propagation at the edges of the slab–wall connections. For that reason, it is more reasonable to model the shear walls and slabs by using finite elements having both flexural and membrane capabilities. Towards this aim, a new nonlinear shell element was developed herein using a nonlinear isoparametric serendipity interpolation scheme with 5 degree of freedom per node. This form of element description was selected in order to have a variable order of displacement definition possible along each of the element edges. This issue is taken up again with details in the forthcoming section.

To reduce the computational time as well as the capacity associated with the 3D modeling of incorporating new shell elements, a mixture of finite elements of different order was used. Higher order finite elements were utilized at the critical locations where the stress concentrations or stress gradients were expected to be high. Therefore, for the five-story building, the first two-story shear walls were simulated with finer mesh. The reinforcements were modeled as discrete or embedded based on the criticality of their locations. The minimum amount of steel percentage taken in the analyses for shear walls and slabs was 0.4% of the section area in accordance with the ACI 318-95 (ACI 1995) specifications. There were also additional longitudinal and diagonal reinforcement used in the modeling in the form of two No. 4 (13 mm in diameter) at the inner and outer faces of the edges, and two No. 4 around the openings, as shown in Fig. 3. The material properties of the concrete and the steel used in the analytical models are presented in Table 1. In the analyses, geometric nonlinearity was disregarded due to the relatively small lateral deformations, whereas, only material nonlinearity was considered as necessary. Possible foundation and soil interaction were ignored, and the shear walls were modeled as sitting on the fixed supports despite that such a support condition may exacerbate the base moments. Effects of the soil–structure interaction on tunnel building performance are the part of our ongoing research.

The loads used in the analyses included the vertical loads due to the live loads, and the dead loads coming from the slabs and shear walls. The lateral forces for the simulation of earthquake loads were calculated as equivalent static loads (i.e., inverted triangle) based on the uniform building code (UBC) (ICBO 1997). The response was computed as the structure was loaded up to its failure using static load increments that were monotonically increased during the pushover analysis. The lateral loading was applied to the story levels simultaneously with the applied gravity loads.

Nonlinear Isoparametric Shell Element

A nonlinear isoparametric shell element providing the capability of a variable edge order and arbitrarily placed movable edge nodes (to consider the location, and amount of main reinforcement near the edges and around the openings as discrete reinforcement) was developed and implemented to *POLO-FINITE* (Dept. of Civil Engineering, Univ. of Illinois, Urbana, Ill.). The rest of the analyses were performed by using this general purpose nonlinear finite element analysis program.

In general, shifting of the edge nodes of the physical element normally causes a node mapping distortion if a standard parent element is used. Unequally spaced nodes results in an unacceptable distortion, therefore some correction techniques for eliminating this distortion were applied using a special mapping between parent element and the physical element (Fig. 4). For that pur-

Table 1. Material Properties for Concrete and Steel

Concrete	Steel	Steel rod element
$E=2.14\times10^6$ t/m^2	$E=2\times10^7$ t/m^2	$E=2\times10^7$ t/m^2
$\nu=0.2$	$\nu=0.3$	$\nu=0.3$
$f_{tu}/f_{cu}=0.06823$	Q_s(top)$=0.2\%$ in both directions	$A_s=0.000226$ m^2 (at openings)
$f_{c28}=1{,}925$ t/m^2	Q_s(bottom)$=0.2\%$ in both directions	$A_s=0.000452$ m^2 (at edges)
	$f_y=22{,}000$ t/m^2	$f_y=22{,}000$ t/m^2

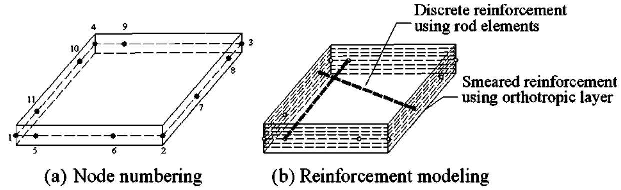

Fig. 5. Nonlinear isoparametric shell element

pose, the standard shape functions and their derivatives normally used for the isoparametric elements were modified for movable edge nodes (El-Mezaini and Citipitioglu 1991). The capability of moving any of the element's edge nodes to any location along an edge allows these edge nodes to be placed in the proper position so that they can serve as end nodes for the cover of the main discrete reinforcement. This provides a robust stiffness contribution coming from the main reinforcement. Besides arbitrarily movable edge nodes, the advantage of a variable edge order in the finite element modeling can be put to good use when the stress gradients are expected to be high. This allows increasing the order of the displacement field in areas such as around openings and in the vicinity of the slab–wall connections (Balkaya and Schnobrich 1993). The matching of the displacement fields between different order finite elements can be adjusted to retain the compatibility along their common edge. To satisfy these conditions during finite element simulations and analyses, an isoparametric shell element having variable edge order and arbitrarily placed edge nodes was developed (Fig. 5).

One of the improvements resulting from the use of this element is the reduction in the capacity and computational time required to reach a solution while retaining the level of accuracy deemed desirable. This concept is essentially important for the case of 3D nonlinear analyses of multistory structures due to their mesh size. In this study, the shape of the stress–strain curve, tension stiffening and the cracking having opening and closing capability (Milford and Schnobrich 1985; Gallegos-Cezares and Schnobrich 1988) were considered in the context of material nonlinearity.

Reinforcement Modeling

Finite element modeling of the reinforcement in a reinforced concrete member can be handled in a number of different ways. The steel can be considered as discrete steel elements, as individual steel units embedded in a concrete element, or as a smeared layer of steel sandwiched within the concrete layers. In the discrete model, reinforcing bars can be modeled using special rod elements located between prescribed element edge nodes. In general, these are two nodded elements which have compatibility discontinuities with the adjacent concrete unit. Higher order elements can be used along the edges of comparable order concrete elements. If a higher order element is desired with the steel placed to pass through the interior of an element, an embedded steel element should be used. On the other hand, the smeared reinforcement model is the easiest to implement and transfers the effects of the steel directly into the concrete elements. In this study, discrete rebars having elasto–plastic stress–strain characteristics were utilized around the openings and near the edges. By using the developed isoparametric shell element, the discrete steel could be easily included while locating the rebars with proper concrete cover requirements. With a two noded rod, the stiffness contributed only to its end nodes. In this case, the bond was neglected due to the incompatible nature of the two displacement fields defining the deformations of the steel and concrete. The smeared steel model was used as the general reinforcement for noncritical locations. It was treated as an equivalent uniaxial layer of the material at the appropriate depth and smeared out over the element as several orthotropic layers. The steel was taken into account in both faces of the slabs and shear walls, and in both principal directions considering the minimum steel ratio and cover thickness.

Crack Modeling

Cracks in concrete can be modeled either as a smeared or a discrete crack model. In the smeared crack modeling, there are several options. They can be modeled either as a fixed crack or as a rotational crack. In most of the finite element analysis of reinforcement concrete structures, crack directions are assumed to be fixed; this means when the crack forms, it remains open. However, this model leads to crack directions that can be inconsistent with the limit state (Gupta and Akbar 1984). The change in the crack direction and the consequential change in the direction of the maximum stiffness were clearly observed in the experiments of Vecchio and Collins (1986). Therefore the need for an algorithm that accounts this rotating crack effect is inevitable. In general, rotating crack models represent the actual behavior more accurately (Milford and Schnobrich 1985). The constitutive matrix used in this study has been derived by Gallegos and Schnobrich (1988). The important concrete cracking behavior was handled through the smeared crack concept that has a rotation, as well as closing and opening capabilities.

Three-Dimensional Effects and Tension–Compression Coupling

Tension–compression (T/C) coupling, executed by in-plane or membrane forces within the shear walls, is a 3D originated mechanism buildup in tunnel form buildings due to the combined effects of wall-to-wall (even including walls with openings) and wall-to-slab interactions (Balkaya and Kalkan 2003b). In this mechanism, the outer walls, oriented perpendicularly to lateral loading directions, act as flanges when subjected to bending loads and resist overall moment primarily in tension and compression. Whereas, the inner walls, passing from the centroid and oriented to the same direction with the lateral loading, act in bending, and their contribution to overall moment capacity are relatively small. In general, this 3D originated mechanism shows a characteristic T-section behavior. Therefore the resultant force mechanism exhibits a significant contribution in the capacity and seismic performance of these buildings. The basic development of T/C coupling mechanism for the tunnel form buildings is presented in Fig. 6.

The analyses showed that the part of the walls above the openings were deflected more in the 2D models than 3D models. During the 2D simulations, the T/C coupling was weakly accomplished with the transverse shear through the coupling beams, whereas, the transverse walls in the 3D cases stiffened the sections by providing additional paths for the shear transfer. The local moment contribution coming from the main walls was not altered significantly between the 2D and 3D cases. This may be attributed to the limitation in the contribution of steel, which is set by the steel area and its yield stress. When the analysis was switched from the 2D to 3D, the transverse walls provided an

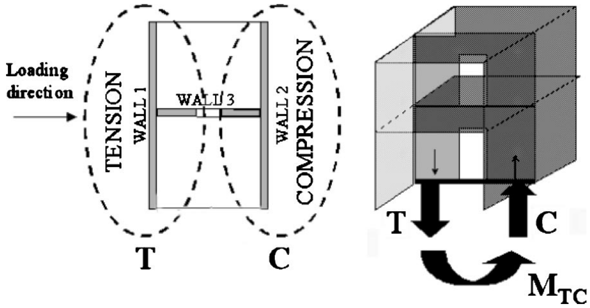

Fig. 6. Slap–wall interaction due to tension and compression (T/C) coupling

extra resistance by substantially increasing the computed lateral load capacity. The total overturning moment capacity of the two-story building at its failure load level was found to be $2,130\ \text{kN m}$ $(213\ \text{t m})$ during the 2D modeling. When the 3D model was considered at this load level, this moment capacity corresponded to $1,703\ \text{kN m}$ $(170.3\ \text{t m})$ and gradually increased up to $4,420\ \text{kN m}$ $(442\ \text{t m})$ at its failure load level. This step up was accredited to the increase in the tension and compression forces that were present in the longitudinal walls and their coupling effects with the transverse walls. A similar behavior was observed for the five-story building as well. Herein, ignoring of possible soil and foundation effects may cause an increase in computed base moments.

Stress Distribution around Openings

Although it is difficult to discern the different patterns of stress concentrations when the magnitudes of the load differs, the general visualizations show that both vertical and shear stress concentrations around the openings in 3D models produced visibly different patterns than 2D models (Figs. 7 and 8). High local vertical stress and shear stress concentrations were observed around the corners of the openings near the edge of the transverse walls. The transverse walls as well as the existing floor slabs in the 3D models strongly affected the stress distribution and stress concentration around the openings. In Fig. 7, comparison of the shear stress distribution at the failure load level of the 2D model [Fig. 7(a)] and the computed shear flow for the 3D model [Fig. 7(b)] corresponds to the failure load level of 2D model are exhibited. The shear force distribution for the 3D model at its failure load level is presented in Fig. 7(c). In these figures, the right portion of Wall 1, including the portion between the openings, carried approximately 60% of the base shear in the 2D case. Whereas, in the 3D models the main shear walls (Wall 1) along the loading direction (y direction) carried most of the total base shear as a membrane shear, while the transverse walls (Wall 2) behaved in flexure by providing their normal shear contributions. Ninety percent of the total base shear was carried by the main shear walls as the membrane forces, and the contribution of the transverse walls in the 3D model was found to be relatively small. The shear capacity of the building increased with the increase in moment resistant capacity. The shear force contribution showed variation as the structure went further in to the nonlinear stage. However, most of the membrane shear was carried by the right portion of Wall 1 in the 3D model, and the present compression zone due to the overturning of the structure provided an effective area for the major shear transfer. For the five-story building, the

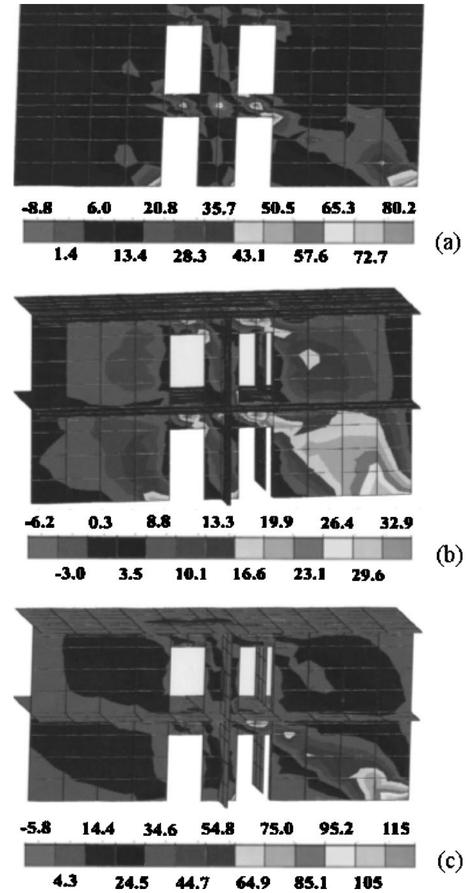

Fig. 7. Shear stress distributions for two-story building (units are in ton meter): (a) two-dimensional model (at failure); (b) three-dimensional model; and (c) three-dimensional model (at failure)

total base shear carried by this portion of the wall increased from 600 kN (60 t) corresponding to the last nonlinear loading step of the 2D model to 1,340 kN (134 t) at the failure load level of the 3D model.

Despite the existence of openings within the transverse walls, they presented high influence on the stress distribution around the

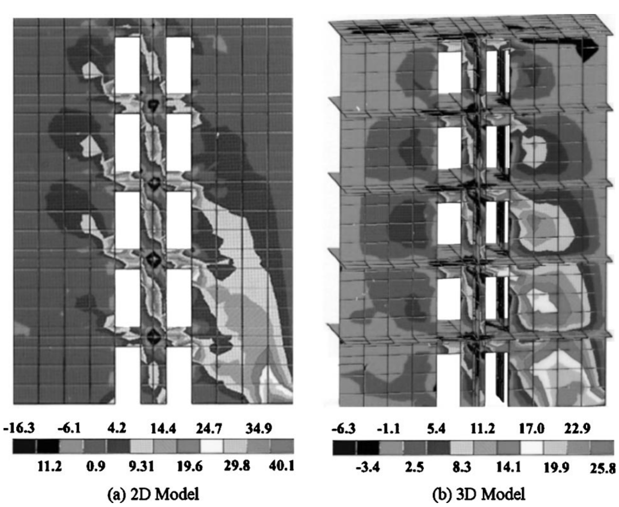

Fig. 8. Shear stress distributions for five-story building (units are in ton meter)

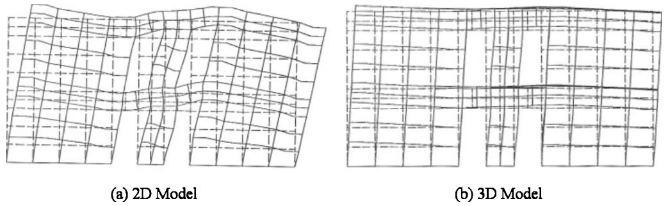

Fig. 9. Deflected shapes for two-story building at failure load level

openings of the main shear walls. The value of the maximum vertical stress carrying capacity at the corners of the openings was increased in the 3D model of the two-story building by about 80% more than that of its 2D model. This desired effect was due to the increase in the computed capacity of the 3D model as it continued to accept more loads. It was further observed that in spite of the openings, introduced a strong disturbance of the shear flow, a strong T/C coupling occurred between the longitudinal and transverse walls.

Strength and Deformation around Openings

The effects of openings on the strength and deformation capacity of the shear wall systems are different than those observed in the conventional frame–wall systems due to the coupling effects of beams connecting the adjacent shear walls. These differences are more evident when the 3D behavior is considered. In general, no contra-flexure points occur above the openings as they do in the 2D coupled wall cases due to the restraint of motion caused by the existing transverse walls and slabs having a continuous edge support in the three dimensions. In this study, the part of the wall between the openings was deflected more in the 2D models than 3D models (Fig. 9). The deflected shapes of two-story building correspond to the last step of pushover analysis before the occurrence of failure. That means excessive crack development at the base level of the shear walls did not yield any more plastic deformation. The crack patterns observed from the 2D and 3D models of the two-story building exhibited significant differentiation at the 2D case failure loading level. However, at the failure load level of the 3D model, the crack patterns turned out to be similar to those observed at the 2D model at failure. The capacity of the main walls was reached at their respective load levels for both cases. Similar observations were obtained for the five-story building, as well. For both case studies, the 2D models resulted in an earlier development and wider propagation of the cracks around the openings. The 2D models showed comparably more bending of the individual walls near the base level than the 3D model. That revealed smaller individual wall bending since its major sections mostly involved in the global bending. The crack patterns for the five-story building around the openings of the upper stories (i.e., above the second story), exhibited similar patterns in both 2D and 3D model. That was basically due to the local stress flow around the openings, and the composite global behavior at the upper levels in the 3D model. It was further observed that the edge and special reinforcement (i.e., diagonal, Fig. 3), including the concrete cover, affected the excessive crack propagation around the openings significantly due to the additional strength they provided.

Slab–Wall Interaction

In order to investigate the effects of slab–wall interaction in the capacity evaluation of tunnel form buildings, a basic model prescribed in Fig. 10 was developed considering the various plans and shear wall configurations. The finite element model was analyzed by conducting a series of 3D nonlinear pushover analyses in a similar fashion as explained before. The analyses were repeated for seven different cases having variable opening dimensions given in Table 2. For the cases of 4a and 4b, Wall 3 was considered as a 12/70 (cm) coupling beam between Wall 1 and Wall 2. Similarly, in the case of 5a and 5b, Wall 3 was totally removed from the model to eliminate the transverse wall effects while providing maximum width and height to the openings. The size and location of the openings, amount of wall reinforcement and discrete reinforcement around the openings were the focal points studied herein in addition to emphasizing to the variable wall configurations, loading directions and distribution of the lateral loads. In order to better illuminate the consequences of slab–wall interaction, the amount of smeared reinforcement incorporated in the walls was increased from 0.2 to 0.5% within the layers near

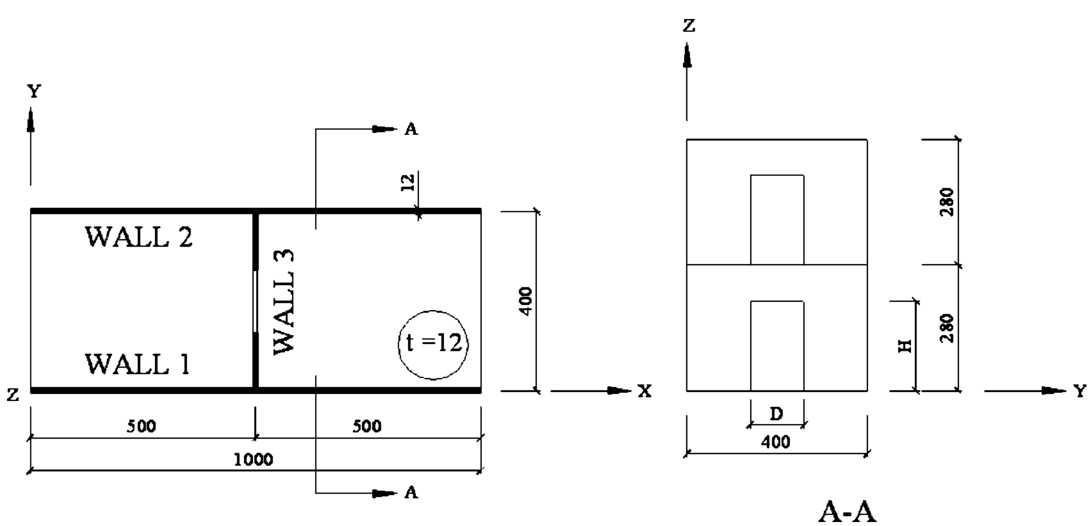

Fig. 10. Typical plan and section view for slab–wall interaction model (units are in cm)

Table 2. Opening Dimensions in Model Structure

Case	Opening size (cm) Width (D)	Height (H)
1	100	210
2	200	210
3	300	210
4a	400	210
4b[a]	400	210
5a	400	280
5b[a]	400	280

[a]Loading condition is different.

the inner and outer faces of the walls and in both horizontal and vertical directions. The number of concrete layers used in the modeling of the walls was also increased to smooth out the nonlinear cracking effects and to better visualize the flexural behavior. In general, cracks at the base of the shear walls developed due to the slab and wall bending moments as well as the moments created by the membrane forces. The lateral loads were applied in the weak direction (y direction) as uniformly distributed forces at the first floor and roof levels. In the case of 4b, the presence of vertical loads was excluded while for the 5b case besides the slab weight, the wall weights were also considered.

The force mechanism developed due to the slab–wall interaction was investigated by focusing on the observed 3D response of the model structures. For the first three cases, the membrane action had the dominant effects on the behavior due to the out-of-plane bending moments in the slabs, which were observed to be smaller than the moments created by the membrane forces. This membrane force couple developed between the forces originated from Wall 1 with the combination of the closer part of Wall 3 and those from Wall 2 with its companion part of Wall 3. These combined parts acted as a T-beam, and local moments due to the membrane forces were calculated considering this T-beam components. Total moment capacities of the models are presented in Fig. 11 with the contribution of the moments created by the slab-bending and membrane forces within the shear walls. For the first three cases, the moments created by the membrane forces within the walls were dominant. With the increase in the size of the opening, this moment contribution from the membrane forces was reduced significantly. In the extreme case (Case 5), the wall bending turned out to be a relatively dominant force mechanism.

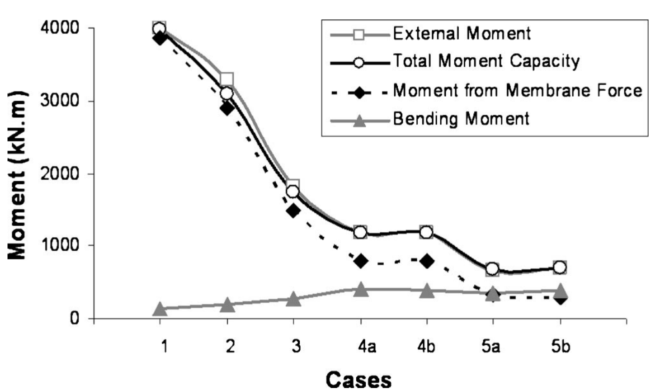

Fig. 11. Distribution of external moment, total computed moment, and its components for seven different cases

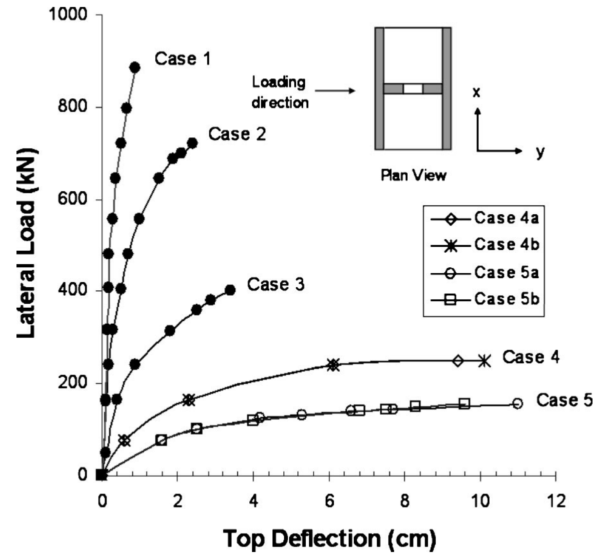

Fig. 12. Load–deflection curves for slab–wall interaction model

The general picture of moment capacity results showed that the membrane moment came only from the T/C coupling forces acting in Walls 1 and 2. The total moment capacity of the structure was reduced from 4,000 kN m (400 t m) to 690 kN m (69 t m) as a consequence of increasing the size of the openings within the interior walls.

The load–deflection curves developed for the studied cases are presented in Fig. 12. The total energy absorption was increased with the increase in the size of the openings (in Wall 3) with the exception of the extreme Case 5. The structures showed more ductile behavior as the lateral deflection increased. The roof displacements especially increased after the formation of the plastic hinges at the base of the structures. Case 1 was observed to behave in a relatively brittle fashion. As no lateral confinement was assumed, first Wall 2 achieved the ultimate compressive strain (ε_{cu}), 0.004. For Cases 4 and 5 the structure behaved in a more flexible manner than the first three cases.

Reinforcement Detailing around Openings

Current codes and design provisions present limited guidelines for the detailing of the reinforcement around the openings of pierced shear walls. The ACI 318-95 Building Code (ACI 1995) does not cover any special reinforcement detailing as was found necessary around the openings. In the commentary of this code, the only available information is related to the shear strength calculation as it depends on the effective cross-sectional area of a wall considering the existing opening. A reasonable estimate for the lower bound of the shear strength of low-rise walls with minimum web reinforcement was presented by Wood in 1990 (Wood 1990). However, the ACI 349-90 Nuclear Safety Structure Code (ACI 1990) [and the UBC (1997)] indicate that in addition to the minimum reinforcement in the walls, not less than two No. 5 (16 mm in diameter) bars shall be provided around the openings. The placement of diagonal shear reinforcement with an angle of 45° at the sections above the openings is recommended in the Turkish Seismic Code (Ministry of Public Works and Settlement 1998).

Due to the formation of high stress concentration around the openings, use of the shear reinforcement as stirrups in the pierced

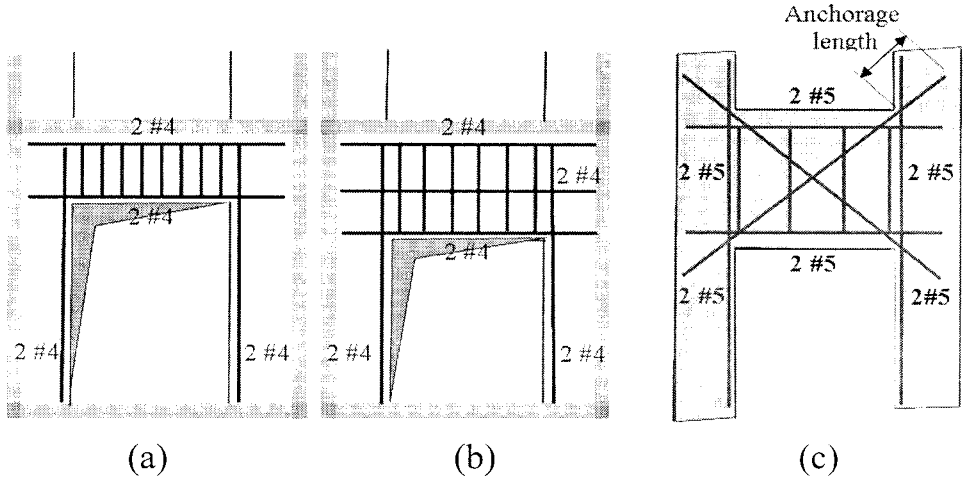

Fig. 13. Reinforcement detailing around openings of pierced shear walls

part in addition to the edge reinforcement provides a significant confinement to the concrete covering the main longitudinal bars, and prevents the buckling of the bars and the premature shear failure. If diagonal bars are not provided, additional shear reinforcement shall be used to resist the diagonal tension. The minimum amount of reinforcement and its detailing shown in Fig. 13(a) can be proposed for pierced shear walls in the case of existence of shallow parts above the openings (using two No. 4 as top and bottom bars, and two No. 4 at each vertical edge). Paulay and Binney (1974) suggested the use of diagonal reinforcement in deep coupling beams because of the relatively large shears that develop and the likelihood of shear failures under reversed seismic loadings, since the deep connections between shear walls in the tunnel form buildings behave in a similar fashion, the reinforcement details given in Figs. 13(b and c) can be suggested when the wall part above the openings of the pierced walls is deeper. It should be noted that connecting beams should not be stronger than its adjacent piers that may cause earlier yielding of piers before deep beams would become inelastic. That further facilitates restricted ductility and poor energy dissipation under seismic excitation, and consequently soft story mechanism may result (Paulay and Priestley 1992). Therefore the degrees of coupling between the wall parts considering the stiffness of the adjacent slabs and transverse walls in the three dimensions should be the basis for the reliable reinforcement detailing around the openings of the tunnel form buildings. The presented reinforcement detailing herein was based on the limited cases investigated; numerous configurations of openings and reinforcement detailing should be evaluated for their generalization.

Conclusions

The results of this study show that both analysis and experimental studies conducted on shear wall dominant buildings without considering the 3D effects of existing transverse walls, as well as the diaphragm flexibilities, may yield inaccurate results. In this study, the stress flow and crack patterns around the openings of pierced shear walls observed through the 3D models were found to be drastically different than those obtained for the 2D models. This was attributed to the nonexistence of contra-flexure points during the 3D behavior. The deflected shapes obtained for the sections above the openings in the 3D models demonstrated more rigid forms than those observed in the 2D models. Considering the interaction effects of the slabs and transverse walls during the analyses increased the overall capacity of the pierced shear walls. It is further observed that despite the existence of openings that introduced a strong disturbance of the shear flow within the transverse walls, these walls provided a significant contribution to the formation of the T/C coupling mechanism during the 3D behavior. However, the magnitude of this contribution was highly affected with the opening size and their locations within the transverse walls.

Even though the membrane action was found to be a dominant force mechanism for the tunnel form building structures, use of developed isoparametric shell element rather than a conventional plane stress element in the finite element models was found to be an effective tool to better represent this mechanism. Besides that use of this element enables various modeling of the reinforcement in the models based on the criticality of their locations. To investigate the local effects around the openings, simulation of reinforcement with discrete elements at such weak locations provided the detail modeling of concrete cover for the development of more realistic crack patterns.

Additionally, due to the nature of high stress concentrations around the openings, use of the diagonal shear reinforcement in addition to the edge reinforcement, may lead significant contribution for retarding and slowing down the crack propagation. The observations and experience gained from this study for the shear wall openings and their impacts on the 3D force mechanism and the general system behavior may help to accomplish more accurate design and analysis of tunnel form buildings as well as to expose their weak and strong points that may remain hidden in the conventional 2D analyses.

References

Ali, A., and Wight, J. K. (1991). "RC structural walls with staggered door openings." *J. Struct. Eng.*, 117(5), 1514–1531.

American Concrete Institute (ACI). (1990). "Commentary on code requirements for nuclear safety related concrete structures." *ACI Manual Part 4, Nuclear Safety Structures Code*, 349-90, Chap. 14.3.4, Detroit, 349–360.

American Concrete Institute (ACI). (1995). "Building code requirements for reinforced concrete and commentary." Committee 318, Detroit, 73–74, 218, 242.

Arvidsson, K. (1974). "Shear walls with door openings near the edge of

the wall." *J. ACI Proc.*, 71(7), 353–357.
Balkaya, C., and Kalkan, E. (2003a). "Nonlinear seismic response evaluation of tunnel form building structures." *Comput. Struct.*, 81, 153–165.
Balkaya, C., and Kalkan, E. (2003b). "Estimation of fundamental periods of shear wall dominant building structures." *Earthquake Eng. Struct. Dyn.*, 32(7), 985–998.
Balkaya, C., and Schnobrich, W. C. (1993). "Nonlinear 3D behavior of shear wall dominant RC building structures." *Struct. Eng. Mech.*, 1(1), 1–16.
Benjamin, J. R., and Williams, H. A. (1958). "Behavior of one-story reinforced concrete shear walls containing openings." *J. ACI Proc.*, 55(5), 605–618.
Daniel, J. I., Shiu, K. N., and Corley, W. G. (1986). "Openings in earthquake-resistant structural walls." *J. Struct. Eng.*, 112(7), 1660–1676.
El-Mezaini, N., and Citipitioglu, E. (1991). "Finite element analysis of prestressed and reinforced concrete structures." *J. Struct. Eng.*, 117(10), 2851–2864.
Gallegos-Cezares, S., and Schnobrich, W. C. (1988). "Effects of creep and shrinkage on the behavior of reinforced concrete gable roof hyperbolic-paraboloids." *Struct. Research Series 543*, UIUC.
Gupta, A. K., and Akbar, H. (1984). "Cracking in reinforced concrete analysis." *J. Struct. Eng.*, 110(8), 1735–1746.
International Conference of Building Officials (ICBO). (1997). Uniform building code, Whittier, Calif.
Kunnath, S. K. (2004). "Identification of modal combinations for nonlinear static analysis of building structures." *Comput. Aided Civ. Infrastruct. Eng.*, in press.
Matsui, G., and Ogawa, T. (1979). "Study on methods of arranging openings in box frame type construction and shearing stress distribution." *Trans. Architectural Institute Japan*, 286, 37–43.
Milford, R. V., and Schnobrich, W. C. (1985). "The application of the rotating crack model to the analysis of reinforced concrete shells." *Comput. Struct.*, 20, 225–234.
Ministry of Public Works and Settlement. (1998). "Specifications for structures to be built in disaster areas." Ankara, Turkey.
Ohtani, H. (1989). "Study of design method of crack width control in openings corner on walls with window openings of reinforced concrete." *J. Struct. Constr. Eng.*, 400, 33–34.
Paulay, T., and Binney, J. R. (1974). "Diagonally reinforced coupling beams of shear walls." *Shear in reinforced concrete, ACI Publication SP-42*, Detroit, 579–598.
Paulay, T., and Priestley, M. J. N. (1992). *Seismic design of reinforced concrete and masonry buildings*," Wiley, New York, 744–799.
Seya, Y., and Matseri, G. (1979). "Study of stress and displacement of shear wall with opening." *Trans. Architectural Institute Japan*, 286, 45–53.
Vecchio, F. J., and Collins, M. P. (1986). "The modified compression-field theory for reinforced concrete elements subjected to shear." *ACI Struct. J.*, 83(2), 219–231.
Yamada, M., Kawamura, H., and Katagihara, K. (1974). "Reinforced concrete shear walls with openings: Test and analysis." *Shear in Reinforced Concrete, Publication SP-42*, ACI, Detroit, 559–578.
Wood, S. L. (1990). "Shear strength of low-rise reinforced concrete walls." *ACI Struct. J.*, 87(1), 99–107.